

# Acrylic AB and ABA Block Copolymers Based on Poly(2-ethylhexyl acrylate) (PEHA) and Poly(methyl methacrylate) (PMMA) via ATRP

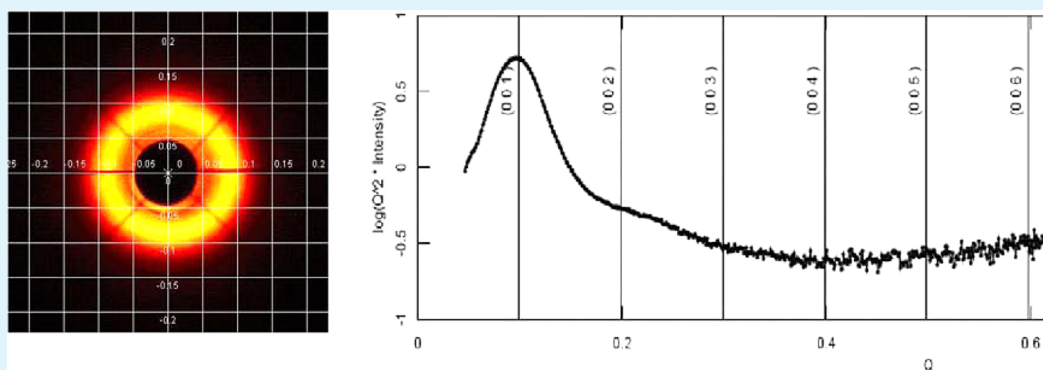
Dhruba J. Haloi,<sup>†</sup> Souvik Ata,<sup>†</sup> Nikhil K. Singha,<sup>\*,†</sup> Dieter Jehnichen,<sup>‡</sup> and Brigitte Voit<sup>‡,§</sup>

<sup>†</sup>Rubber Technology Centre, Indian Institute of Technology Kharagpur, Kharagpur-721302, India

<sup>‡</sup>Leibniz-Institute of Polymer Research Dresden, Hohe Strasse 6, D-01069 Dresden, Germany

<sup>§</sup>Organic Chemistry of Polymers, Technische Universität Dresden, 01062, Dresden, Germany

## S Supporting Information



**ABSTRACT:** Acrylic block copolymers have several advantages over conventional styrenic block copolymers, because of the presence of a saturated backbone and polar pendant groups. This investigation reports the preparation and characterization of di- and triblock copolymers (AB and ABA types) of 2-ethylhexyl acrylate (EHA) and methyl methacrylate (MMA) via atom transfer radical polymerization (ATRP). A series of block copolymers, PEHA-*block*-PMMA (AB diblock) and PMMA-*block*-PEHA-*block*-PMMA (ABA triblock) were prepared via ATRP at 90 °C using CuBr as catalyst in combination with N,N,N',N'',N'''-pentamethyl diethylenetriamine (PMDETA) as ligand and acetone as additive. The chemical structure of the macroinitiators and molar composition of block copolymers were characterized by <sup>1</sup>H NMR analysis, and molecular weights of the polymers were analyzed by GPC analysis. DSC analysis showed two glass transition temperatures ( $T_g$ ), indicating formation of two domains, which was corroborated by AFM analysis. Small-angle X-ray scattering (SAXS) analysis of AB and ABA block copolymers showed scattering behavior inside the measuring limits indicating nanophase separation. However, SAXS pattern of AB diblock copolymers indicated general phase separation only, whereas for ABA triblock copolymer an ordered or mixed morphology could be deduced, which is assumed to be the reason for the better mechanical properties achieved with ABA block copolymers than with the AB analogues.

**KEYWORDS:** atom transfer radical polymerization (ATRP), 2-ethylhexyl acrylate (EHA), morphology, block copolymer, mechanical properties, thermoplastic elastomer (TPE)

## INTRODUCTION

Block copolymers are interesting materials, which have applications as emulsifier, adhesive, and in biomedical carrier systems, but also as bulk material with special properties, for examples, as thermoplastic elastomer (TPE).<sup>1</sup> The properties of block copolymers can be controlled by designing the length and the nature of their blocky segments, like soft–hard, hydrophilic–hydrophobic, ionic–nonionic segments etc.<sup>2–6</sup> Self-assembling of block copolymers can lead to nanostructured material.<sup>7</sup> Conventional styrene based block copolymers for bulk application (like SBS, SEBS, SEPS etc.) have several disadvantages, e.g., poor resistance to weatherability, oxidative degradation, UV light, and fuels.<sup>8</sup> Having a saturated backbone and a polar pendant group, acrylic elastomers have very good resistance to heat, oxidative/ozonolytic degradation, oils and

fuels.<sup>1,8</sup> Acrylic block copolymers have interesting properties that can be tuned by using different acrylate monomers as well as by manipulating their block length.<sup>9–15</sup> These properties can be tailored through the combination of a hard segment in terms of methacrylate block of high  $T_g$  with a soft segment of low  $T_g$  acrylate block. In ABA-type triblock copolymer, if A and B blocks are properly tuned that A-block can form hard domains and B-block can act as soft domain, then the block copolymer can have interesting morphology and properties.<sup>16–18</sup> The appropriate composition of both A and B may lead to a thermoplastic elastomeric polymer (TPE) which can have

Received: May 22, 2012

Accepted: July 26, 2012

Published: July 26, 2012

different potential applications.<sup>19,20</sup> During last two decades there have been overwhelming developments in the field of controlled radical polymerization (CRP) which has the versatility of a radical polymerization and the controlled/living character of ionic polymerization. Among different types of CRP, atom transfer radical polymerization (ATRP) is a very versatile technique that is tolerant to different functionalities present in the monomer and in the initiator. ATRP leads to very high molecular weight block copolymer. Therefore, ATRP has been used extensively now-a-days to prepare different all acrylic block copolymers based on poly(meth)acrylate.

The preparation of AB and ABA types of block copolymers based on acrylates having a long chain pendent alkyl group has been reported.<sup>21,22</sup> All acrylic block copolymers based on octadecyl acrylate,<sup>23</sup> octadecyl methacrylate,<sup>24</sup> hexyl acrylate,<sup>25</sup> lauryl acrylate<sup>26</sup> have been reported by several research groups. Poly(2-ethylhexyl acrylate) (PEHA) has branched alkyl chains and has very good film formation property, because of which it is an important component in paints and coating application. Acrylic block copolymers based on PEHA and PMMA can have potential applications as TPE in which PMMA can act as hard segment and PEHA block can act as soft segment, because of its relatively low  $T_g$  ( $-65$  °C). These block copolymers may be potential materials for outdoor applications, oil resistant paints and coatings or in automotive parts. There is so far no report on the preparation, properties and morphological characterizations of all acrylic block copolymers based on PEHA and PMMA.

This investigation reports preparation and characterization of all acrylic di- and triblock copolymers (AB and ABA types) based on PEHA and PMMA via atom transfer radical polymerization (ATRP). The prepared block copolymers were characterized by GPC and <sup>1</sup>H NMR analyses. Mechanical properties were evaluated by using universal testing machine (UTM). DSC, AFM, TEM, and SAXS analyses confirmed the nanophase separated morphology in these block copolymers.

## ■ EXPERIMENTAL SECTION

**Materials.** 2-Ethylhexylacrylate (EHA) (98%, Aldrich; USA) and methyl methacrylate (MMA) (98%, Aldrich; USA) were purified by passing through alumina (basic) packed column. CuBr (99.9%, Aldrich; USA) was purified by washing with glacial acetic acid followed by diethyl ether and finally was dried under vacuum. Acetone (Merck) was purified by distillation under reduced pressure. N,N,N',N'-pentamethyl diethylenetriamine (PMDETA) (99%, Aldrich; USA), tetrahydrofuran (THF) (Merck), dichloromethane (Merck), triethylamine (Merck), methyl 2-bromopropionate (98%, Aldrich; USA), and 2-bromoisobutyl bromide (98%, Aldrich; USA) were used as received.

**Polymerization Procedure. Preparation of Monofunctional Macroinitiator (PEHA-Br).** ATRP of EHA was carried out in a Schlenk tube at 90 °C to prepare macroinitiator for block copolymerization with MMA. In this polymerization reaction, the catalyst, CuBr (0.0688 g;  $4.8 \times 10^{-4}$  mol) was taken in a Schlenk tube and was sealed with a silicone rubber septum. Nitrogen was purged through it for 10 min to expel out the oxygen present inside the Schlenk tube. The ligand PMDETA (0.125 g;  $7.21 \times 10^{-4}$  mol) and methyl 2-bromopropionate (MBrP) (0.0803 g;  $4.81 \times 10^{-4}$  mol) were dissolved in acetone (4 mL) and was transferred to the Schlenk tube with continuous purging of nitrogen. EHA (20 mL,  $9.62 \times 10^{-2}$  mol) was then introduced to the mixture. The Schlenk tube was then immersed into an oil bath already heated at 90 °C to start the polymerization reaction. The polymerization was run for 3 h and the prepared poly(2-ethylhexyl acrylate) was purified by diluting with THF followed by reprecipitating from methanol. Yield = 15.7 g; conversion = 90%;  $M_{n(\text{Theo})} = 33100$  g mol<sup>-1</sup>;  $M_{n(\text{GPC})} = 37000$  g mol<sup>-1</sup>; PDI = 1.20.

### Preparation of AB-Type Diblock Copolymer (PEHA-*b*-PMMA).

The prepared monofunctional macroinitiator was used to prepare AB-type diblock copolymers with MMA. In a typical block copolymerization reaction, macroinitiator (PEHA-Br) (2.18 g;  $M_n = 37000$ ; PDI = 1.20) was taken in a Schlenk tube. CuBr (0.0074 g;  $5.17 \times 10^{-5}$  mol) was then added to the Schlenk tube and the tube was sealed with a rubber septum. Nitrogen was purged through the reaction system for 10 min to expel out the oxygen present inside the reaction tube. PMDETA (0.0135 g;  $7.78 \times 10^{-5}$  mol) in acetone (1 mL) was then introduced to the Schlenk tube with the help of a syringe. On continuous stirring, monomer MMA (4 mL;  $3.73 \times 10^{-2}$  mol) was added to the reaction mixture. The reaction was started by putting the Schlenk tube in the oil bath preheated at 90 °C. After 2 h of reaction time the Schlenk tube was removed from the oil bath. The diblock copolymer thus prepared was diluted with THF and purified by reprecipitating from methanol. The purified diblock copolymers were characterized by different techniques for property evaluation. Conversion = 80%;  $M_{n(\text{Theo})} = 85000$  g mol<sup>-1</sup>;  $M_{n(\text{GPC})} = 87000$  g mol<sup>-1</sup>; PDI = 1.40.

**Preparation of Bifunctional Initiator and Macroinitiator (Br-PEHA-Br).** The bifunctional initiator, 1,2-bis(bromoisobutyryloxy) ethane (bBr-iBE) was prepared by a simple esterification reaction between ethylene glycol and 2-bromoisobutyl bromide.<sup>27</sup> This bifunctional initiator was then used to prepare bifunctional macroinitiator based on PEHA (Br-PEHA-Br) using the same procedure as explained for monofunctional macroinitiator (PEHA-Br). The polymerization reaction was carried out in Schlenk tube. The different ingredients used were; bifunctional initiator (bBr-iBE) (0.1731 g;  $4.81 \times 10^{-4}$  mol), CuBr (0.1376 g;  $9.62 \times 10^{-4}$  mol), PMDETA (0.25 g;  $1.44 \times 10^{-3}$  mol) in acetone (4 mL) and monomer EHA (20 mL;  $9.62 \times 10^{-2}$  mol). The polymerization reaction was carried out at 90 °C for 2 h. The prepared bifunctional macroinitiator (Br-PEHA-Br) was purified by dissolving in THF and reprecipitating from methanol. Yield = 13.1 g; conversion = 75%;  $M_{n(\text{Theo})} = 27600$  g mol<sup>-1</sup>;  $M_{n(\text{GPC})} = 29000$  g mol<sup>-1</sup>; PDI = 1.26.

**Preparation of ABA-Type Triblock Copolymer (PMMA-*b*-PEHA-*b*-PMMA).** The bifunctional macroinitiator (Br-PEHA-Br) ( $M_n = 29000$ ; PDI = 1.26) prepared via the method explained earlier was used to prepare ABA-type triblock copolymers with MMA (PMMA-*b*-PEHA-*b*-PMMA) using the same procedure as adopted for AB diblock copolymers. In this case different ingredients used were; bifunctional macroinitiator (Br-PEHA-Br) (2.17 g;  $7.48 \times 10^{-5}$  mol), CuBr (0.0066 g;  $4.61 \times 10^{-5}$  mol), PMDETA (0.0121 g;  $6.98 \times 10^{-5}$  mol), acetone (1 mL) and monomer MMA (6 mL;  $2.89 \times 10^{-2}$  mol). The final polymer was purified by redissolving in THF and reprecipitating from methanol. Conversion = 73%;  $M_{n(\text{Theo})} = 55000$  g mol<sup>-1</sup>;  $M_{n(\text{GPC})} = 57000$  g mol<sup>-1</sup>; PDI = 1.38.

**Characterization. GPC Analysis.** The molecular weights ( $M_n$ ) of the macroinitiators and the block copolymers were measured at ambient temperature by Size Exclusion Chromatography (SEC) on a VISCOTEK, GPC instrument equipped with two ViscoGel mix bed columns (17360-GMHHRM) connected in series with a refractive index detector model, VE 3580 RI detector. THF was used as eluent at a flow rate of 1 mL/min. Poly (methyl methacrylate) standards of narrow polydispersity index (PDI) were used as calibration standard. Data analysis was collected using OmniSEC 4.2 software. Waters SEP-Pak cartridges were used to remove Cu salts from the polymers before injecting into the GPC system.

**NMR Spectroscopy.** <sup>1</sup>H NMR spectra were recorded on 200 MHz (Bruker) NMR spectrometer using CDCl<sub>3</sub> as solvent containing a small amount of TMS as internal standard. The molar composition in the block copolymers was calculated from these <sup>1</sup>H NMR spectra.

**Thermal Analysis.** Differential scanning calorimetry (DSC) analysis was carried out on a TA (DSC Q100 V8.1 Build 251) instrument at a heating rate of 10 °C/min under nitrogen atmosphere. In this case, the sample was heated to +150 °C then cooled to -100 °C. The sample was again heated to +150 °C at the heating rate of 10 °C/min. The second heating cycle curve was used to calculate the  $T_g$  of the polymers. Thermogravimetric analysis (TGA) was carried out on a TA (TGA Q50 V6.1 Build 181) instrument. In this case, a small amount of

sample (approximately 8 mg) was heated from room temperature to 600 °C at a heating rate of 10 °C/min under nitrogen atmosphere.

**Tensile Property.** The block copolymers were solution cast to prepare a sheet which was cut into test specimens (type V) according to ASTM standard, ASTM D638–08. The tensile testing was carried out in a Hioks–Hounsfield Universal Testing Machine (Test Equipment, Ltd., Surrey, England) according to ASTM D638–08 test method using dumbbell shaped specimen (type V) at a cross-head speed of 100 mm/min at room temperature ( $25 \pm 1$  °C). The average of three analysis has been reported here.

**Atomic Force Microscopy (AFM).** The topographic phase images of polymers were recorded using atomic force microscopy (AFM) (Nanonics Imaging Ltd. Malcha, Jerusalem, Israel) in tapping mode. Thin polymer films of ~500 nm thickness were cast on mica foil from a dilute polymer solution (2 mg/mL) in THF followed by slow evaporation of solvent. The changes in surface topography were measured quantitatively by root-mean-square (rms) roughness ( $R_q$ ), roughness average ( $R_a$ ), and ( $R_q - R_a$ ) calculation.

**Small-Angle X-ray Scattering (SAXS).** The film samples prepared for tensile measurements were also used for the SAXS analysis. In this case the film samples were prepared using solvent casting method. About 10% (w/v) solution of block copolymer in THF was prepared for this. The SAXS analysis was carried out on solid films using three pinhole collimation system with Rigaku rotating anode generator (40 kV, 30 mA, Cu–K $\alpha_n$  radiation). The SAXS 2D patterns were recorded within scattering range of  $q \sim 0.05$  to  $1.0 \text{ nm}^{-1}$  using area detector system marCCD (Mar USA, Inc., detector resolution  $\sim 79 \mu\text{m}$ ). SAXS diffractograms were calculated as Lorentz corrected scattering curves ( $Iq^2$ ) by sectoral integration over total azimuthal range due to isotropic scattering.

**UV–Vis Spectroscopy.** The transmittance spectrum of the ABA block copolymer film of thickness about 0.5 mm was recorded at room temperature in a Spectrascan UV 2600 digital spectrophotometer (Chemito, India) inserting the film into a 1 cm well-stopper quartz cuvette.

## RESULTS AND DISCUSSION

**Synthesis and Characterization of AB Diblock and ABA Triblock Copolymers.** ABA and AB type block copolymers were prepared via ATRP at 90 °C using CuBr as catalyst in combination with PMDETA as ligand. For the ABA type block copolymer, at first the bifunctional macroinitiator Br-PEHA-Br was prepared using bBr-iBE as bifunctional initiator, CuBr as catalyst in combination with PMDETA as ligand in presence of a small amount of acetone. Addition of small amount of polar solvent has beneficial effects in the ATRP of acrylates having long chain.<sup>25,28</sup> See Figure S1 in the Supporting Information shows the  $^1\text{H}$  NMR spectrum together with the assignment of different protons in the bifunctional macroinitiator (Br-PEHA-Br). A small resonance at  $\delta = 4.4$  ppm (designated as 7 in Figure S1 in the Supporting Information) is due to the proton attached to the terminal –Br group which indicates that the bifunctional macroinitiator has the desired bromo end groups. The resonances at  $\delta = 3.8$  ppm were due to the –OCH<sub>2</sub>– protons of the alkyl pendant group in PEHA. The molecular weight of the macroinitiator was determined by comparing the resonances at  $\delta = 4.4$  ppm for >CH-Br of the end group and  $\delta = 3.8$  ppm (for –OCH<sub>2</sub>–) protons in PEHA. However, in this case the integral area of two –OCH<sub>2</sub>– protons of bifunctional initiator (bBr-iBE) was taken into consideration while calculating the  $M_{n,\text{NMR}}$  of Br-PEHA-Br. The activity as a bifunctional macroinitiator was further confirmed by a chain extension experiment. In this experiment, the bifunctional macroinitiator (Br-PEHA-Br) was used to polymerize a second monomer to prepare ABA type triblock copolymer (Br-PMMA-*b*-PEHA-*b*-PMMA-Br). Figure 1 shows

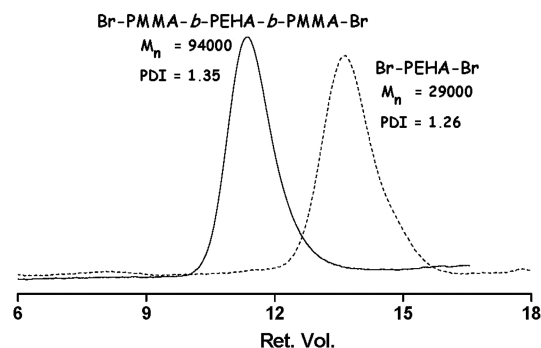


**Figure 1.** GPC traces of bifunctional macroinitiator (Br-PEHA-Br) and triblock copolymer.

the complete shift of the GPC traces after chain extension toward higher molecular weight region (lower elution volume). This confirms the living nature of the –Br end group in the macroinitiator. Figure 2 shows the  $^1\text{H}$  NMR spectra of an ABA type triblock copolymer. The various protons present in the block copolymer with their designations are shown in the Figure 2. The characteristic peak at  $\delta = 4.0$  ppm is due to two protons (–OCH<sub>2</sub>–) (designated as 1 in Figure 2) of the 2-ethylhexyl acrylate part. Another characteristic peak at  $\delta = 3.6$  ppm is due to the three protons (–OCH<sub>3</sub>) (designated as 7 in Figure 2) present in the PMMA part. The molar composition of PMMA was calculated by using the following equation.

$$M_{\text{MMA}} = \frac{2A}{2A + 3B} \times 100\% \quad (1)$$

Where  $M_{\text{MMA}}$  is the molar percentage of MMA in the block copolymer. A and B are the area under the peaks designated as 7 and 1, i.e., for –OCH<sub>3</sub> and –OCH<sub>2</sub>– protons, respectively, as shown in Figure 2. Molecular weights and the molar composition of different ABA block copolymers are shown in Table 1. They indicate that the prepared ABA-type triblock copolymers have narrow molecular weight distributions and the molecular weights were almost equal to  $M_{n,\text{theo}}$ . It was observed that the molecular weight distribution of triblock copolymer was relatively narrow in case of longer PMMA blocks compared to shorter PMMA blocks. It indicates that with increasing the PMMA block (with increased polymerization time), i.e., in the block copolymer of higher molecular weight there was no loss in control during the block copolymerization.

The AB type block copolymer was prepared via ATRP of MMA using the monofunctional poly(2-ethylhexyl acrylate) (PEHA-Br) macroinitiator at 90 °C in the presence of CuBr as catalyst in combination with PMDETA as ligand. In this case, a series of AB-type diblock copolymers with different PMMA length was prepared varying the amount of the second monomer, MMA, in the feed. In GPC analysis, the complete shift of GPC traces toward higher molecular weight region (see Figure S2 in the Supporting Information) and the presence of new resonances at  $\delta = 3.5$  ppm due to –OCH<sub>3</sub> protons in the PMMA segment ( $^1\text{H}$ NMR spectrum of diblock copolymer is shown in Figure S3 in the Supporting Information) in addition to the resonances at  $\delta = 4.2$  ppm due to –OCH<sub>2</sub>– protons in PEHA-Br macroinitiator indicate the successful block copolymer formation. The chemical composition of the AB block copolymer was determined from the resonances at  $\delta = 3.5$  ppm (in PMMA) and  $\delta = 4.2$  ppm (in PEHA) by using the eq 1, as performed in ABA block copolymer. Table 2 summarizes the molecular weights and the molar composition of the AB

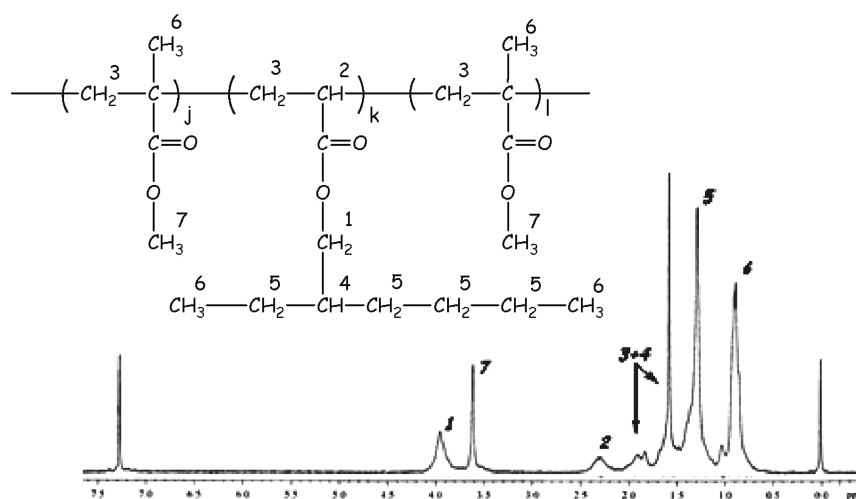


Figure 2.  $^1\text{H}$  NMR spectrum of PMMA-*b*-PEHA-*b*-PMMA triblock copolymer.

Table 1. ABA-Type Triblock Copolymers (PMMA-*b*-PEHA-*b*-PMMA) via ATRP Using Br-PEHA-Br as Bifunctional Macroinitiator<sup>a</sup>

sample	block length		PMMA- <i>b</i> -PEHA- <i>b</i> -PMMA						
	PEHA (g mol <sup>-1</sup> )	PMMA (g mol <sup>-1</sup> )	$M_{n(\text{Theo})}$ (g mol <sup>-1</sup> )	$M_{n(\text{GPC})}$ (mol <sup>-1</sup> )	$M_{n(\text{NMR})}^c$ (g mol <sup>-1</sup> )	PDI	EHA <sup>b</sup> (mol %)	MMA <sup>b</sup> (mol %)	
ABA-1	29k	6k	39k	41k	43k	1.40	53.3	46.7	
ABA-2	29k	14k	55k	57k	60k	1.38	33.3	66.7	
ABA-3	29k	31k	87k	91k	92k	1.35	20.1	79.9	

<sup>a</sup>Bifunctional macroinitiator Br-PEHA-Br has  $M_{n(\text{GPC})} = 29\,000$  g mol<sup>-1</sup>; PDI = 1.26 <sup>b</sup>Molar composition is measured by  $^1\text{H}$  NMR analysis

<sup>c</sup>Molecular weight was calculated using mol % obtained from  $^1\text{H}$  NMR analysis

Table 2. AB-Type Diblock Copolymers (PEHA-*b*-PMMA) via ATRP Using PEHA-Br as Monofunctional Macroinitiator<sup>a</sup>

sample	block length		PEHA- <i>b</i> -PMMA						
	PEHA (g mol <sup>-1</sup> )	PMMA (g mol <sup>-1</sup> )	$M_{n(\text{Theo})}$ (g mol <sup>-1</sup> )	$M_{n(\text{GPC})}$ (g mol <sup>-1</sup> )	$M_{n(\text{NMR})}^c$ (g mol <sup>-1</sup> )	PDI	EHA <sup>b</sup> (mol %)	MMA <sup>b</sup> (mol %)	
AB-1	37k	8k	42k	45k	48k	1.50	63.3	36.7	
AB-2	37k	25k	60k	62k	68k	1.48	39.1	60.9	
AB-3	37k	32k	66k	69k	74k	1.43	35.2	64.8	
AB-4	37k	50k	85k	87k	90k	1.40	27.4	72.6	

<sup>a</sup>Macroinitiator PEHA-Br has  $M_{n(\text{GPC})} = 37\,000$  g mol<sup>-1</sup>; PDI = 1.20 <sup>b</sup>Molar composition is measured by  $^1\text{H}$  NMR analysis <sup>c</sup>Molecular weight was calculated using mol % obtained from  $^1\text{H}$  NMR analysis

Table 3. Thermal Properties of ABA Triblock and AB Diblock Copolymers

sample	block length		copolymer composition (mol %)		$T_g$ (1) (°C)	$T_g$ (2) (°C)	$T_{\text{onset}}^a$ (°C)	$T_{\text{max}}$ (°C)
	PEHA	PMMA	EHA	MMA				
ABA-1	29k	6k	53.3	46.7	-65	127	296	370
ABA-2	29k	14k	33.3	66.7	-65	131	287	377
ABA-3	29k	31k	20.1	79.9	-65	129	279	374
AB-2	37k	25k	39.1	60.9	-66	122	291	376
AB-4	37k	50k	27.4	72.6	-66	124	262	366

<sup>a</sup> $T_{\text{onset}}$  is calculated at 5% weight loss from the TGA curve.

diblock copolymers of EHA and MMA. The block copolymers had PEHA contents of 27 mol % to 64 mol % and the molecular weights of the block copolymers were comparable with the theoretical molecular weights.

**Thermal Properties of AB Diblock and ABA Triblock Copolymers.** Glass transition temperature ( $T_g$ ) of the block copolymers was determined by DSC analysis. The DSC plots of the ABA triblock copolymers with different PMMA length are shown in Figure S4 in the Supporting Information. DSC

analysis showed two  $T_g$ 's in the ABA triblock copolymers PMMA-*b*-PEHA-*b*-PMMA (see Figure S4 in the Supporting Information). The  $T_g$  at around 127 °C is for the hard PMMA segment and the  $T_g$  at -65 °C is due to the soft PEHA part of the triblock copolymers. The  $T_g$  values of the triblock copolymers are shown in Table 3. The presence of two  $T_g$ 's indicates the formation of two types of domains: hard domains of PMMA and soft domains of PEHA in the ABA type triblock copolymer. Glass transition temperatures of the diblock

copolymers were also determined by DSC analysis. All the diblock copolymers showed similar two  $T_g$ s; one at  $-66\text{ }^\circ\text{C}$  and another at around  $122\text{ }^\circ\text{C}$  (Table 3, Figure S5 in the Supporting Information) indicating also the formation of hard and soft domain in the AB block copolymer. There was increase in  $T_g$  of PMMA block in the block copolymer compared to the  $T_g$  of PMMA homopolymer.<sup>31,32</sup> The increase in the  $T_g$  of the PMMA block has also been reported in the nanophase-separated, all-acrylic block copolymers of PMMA.<sup>33,34</sup>

Thermogravimetric analysis of the block copolymers were carried out to study their thermal stability. The TGA and DTG thermograms of different triblock copolymers are shown in Figure S6 in the Supporting Information. Table 3 summarizes the TGA data of the triblock copolymers. It indicates that  $T_{\text{onset}}$  (temperature at 5 wt % loss) and  $T_{\text{max}}$  (maximum decomposition temperature) decreased slightly with increasing PMMA length. This is probably due to the easier degradation of PMMA part, as its tertiary carbon is more prone to thermal degradation. A similar trend in  $T_{\text{onset}}$  and  $T_{\text{max}}$  was also observed in TGA analysis of AB diblock copolymers (Table 3). (TGA and DTG thermograms of AB diblock copolymer are shown in Figure S7 in the Supporting Information).

**Tensile Property of AB Diblock and ABA Triblock Copolymers.** Tensile properties of diblock copolymers were evaluated using a universal testing machine as explained in the Experimental Section. Figure 3 shows the stress–strain plots of

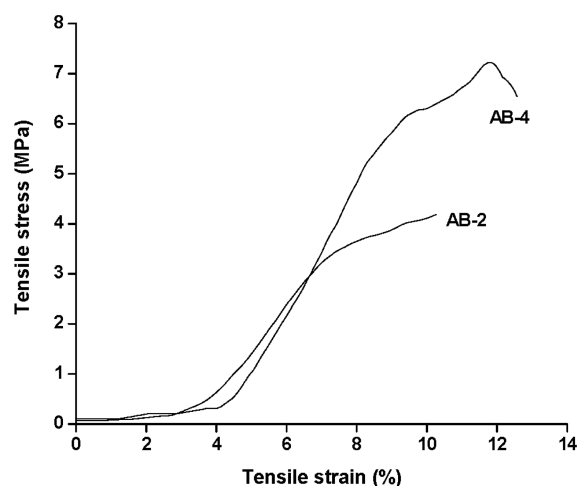


**Figure 3.** Stress–strain plots of AB type diblock copolymers of EHA and MMA.

**Table 4. Tensile Properties of AB and ABA Block Copolymers**

sample	block length		copolymer composition (mol %)		tensile strength (MPa)	elongation at break (%)
	PEHA	PMMA	EHA	MMA		
AB-2	37k	25k	39.1	60.9	$4.1 \pm 0.40$	$10.2 \pm 0.45$
AB-4	37k	50k	27.4	72.6	$7.2 \pm 0.88$	$12.5 \pm 0.62$
ABA-2	29k	14k	33.3	66.7	$15.9 \pm 0.41$	$44.6 \pm 0.55$
ABA-3	29k	31k	20.1	79.9	$17.4 \pm 0.45$	$15.8 \pm 0.26$

diblock copolymers and Table 4 summarizes the mechanical properties. Like most of the elastomers, these samples show some initial strain, before there is an increase in stress on increasing strain. The tensile strength was found to increase with increase in PMMA length. This is expected, as PMMA part acts as hard domain and reinforces the mechanical properties. However, there was a further drastic increase in the mechanical properties going from AB di-block copolymers to ABA type triblock copolymers (Figure 4, Table 4). With almost similar

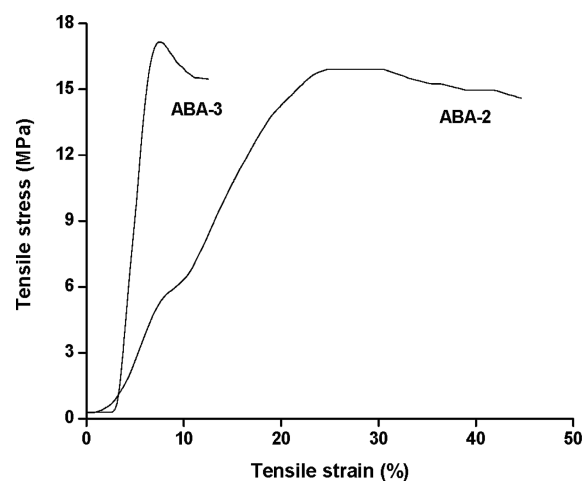


**Figure 4.** Stress–strain plots of ABA-type triblock copolymers of EHA and MMA.

PMMA content, the tensile strength in ABA block copolymer is much greater than in the AB block copolymer. For example, with 61 mol % PMMA content and with a PMMA block length of 25000 g/mol, AB-1 block copolymer shows a tensile strength of only 4.1 MPa (Table 4). But ABA-2 block copolymer with 66 mol % PMMA content and two 7000 g/mol PMMA blocks shows a tensile strength of 16 MPa, about four times greater than the AB-1 diblock copolymer. Furthermore, as expected, the elongation at break decreases in the ABA triblock copolymers with increasing PMMA content, a typical effect of reinforcing hard domains, which is not observed for the AB diblock copolymers. This indicates that the tensile properties of the block copolymers do not depend solely on the PMMA content, though it acts as reinforcing segment and thus, it can be assumed that a much more effective morphology is achieved for the ABA triblock copolymers compared to the AB block copolymers. The stress–strain plot of ABA-2 block copolymer seems to show a first yield point at a low strain (10%) and second yield point at higher strain. Ward et al.<sup>35</sup> reported double yield points in polyethylenes having different branch content. They observed that the first yield point at low applied strains which indicates the onset of temporary deformation. The second yield point occurs at higher strain which marks the onset of permanent deformation. So we speculate that in the present ABA-2 block copolymer the first yield at 10% strain may be due to the different temporary morphology due to longer branched alkyl pendant group in PEHA followed by the second yield at higher strain before the breaking point. ABA-3 having higher PMMA content (79.9%) showed different behavior. It showed necking behavior that is a characteristic of thermoplastic materials.<sup>36,37</sup>

**Morphology of the Block Copolymers. AFM Analysis of Block Copolymers.** Figure 5 shows the tapping mode phase

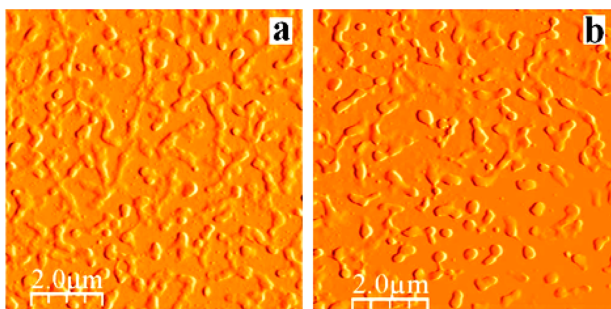


**Figure 5.** AFM phase images of (a) AB (AB-4) type diblock copolymer, (b) ABA (ABA-2) type triblock copolymer.

atomic force microscopy (AFM) images of the block copolymers prepared as thin film from THF solution. They show distinct nanophase separation. It was also observed that nanodomains were continuously dispersed in the matrix and no major differences can be deduced between the AB and ABA block copolymer.

**Small-Angle X-ray Scattering (SAXS) of Block Copolymers.** The block copolymers prepared as solid films were also analyzed by small-angle X-ray scattering (SAXS) analysis. SAXS patterns of AB and ABA block copolymers are shown in panels a and b in Figure 6, respectively. Figure 6c shows the SAXS intensity vs  $q$  profiles of AB type diblock and ABA type triblock copolymers of EHA and MMA. SAXS patterns of AB and ABA block copolymers showed scattering behavior inside the measuring limits indicating nanophase separation. Only one

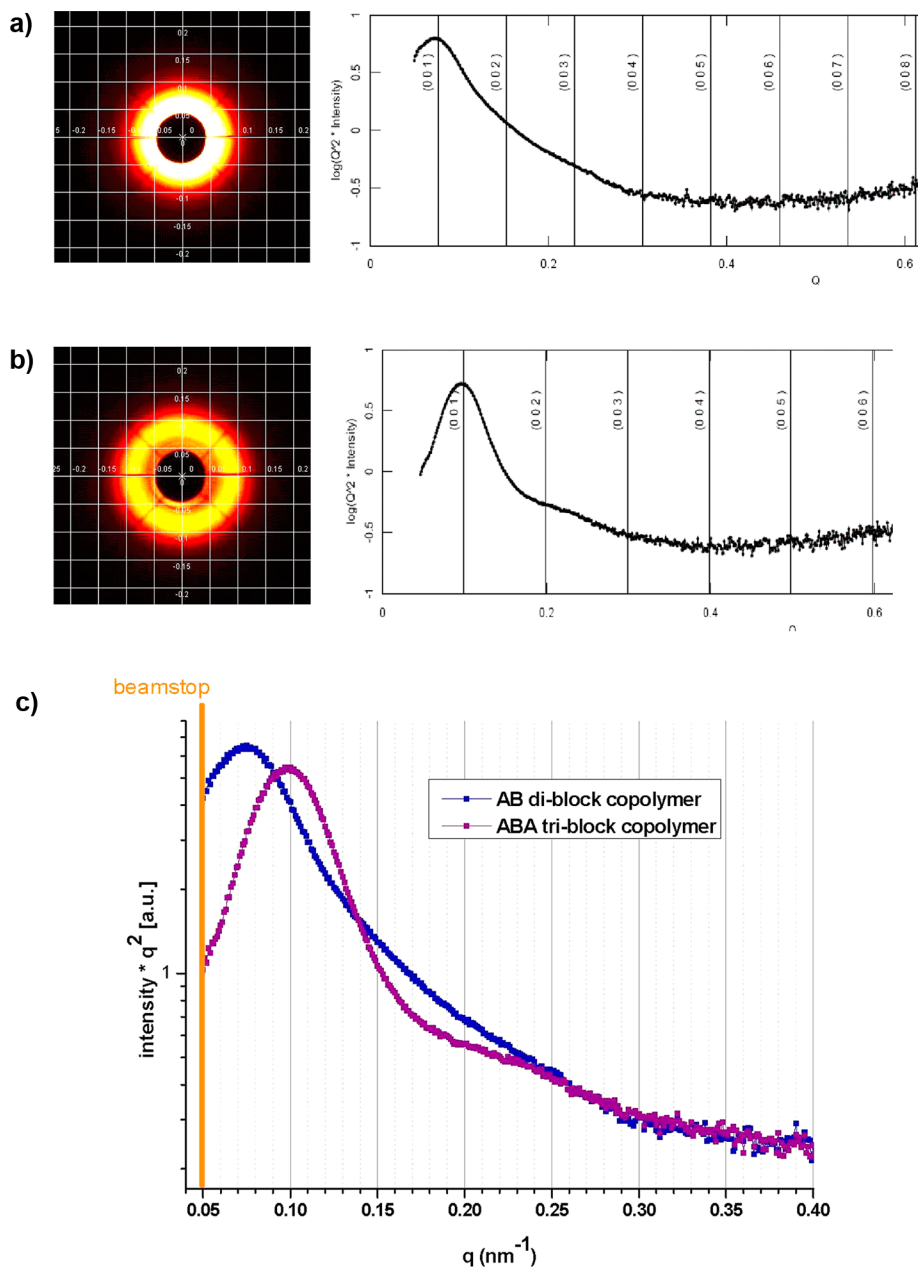


**Figure 6.** (a) 2D-pattern (mesh width:  $\Delta q = 0.05 \text{ nm}^{-1}$ ) for AB (AB-4) type diblock copolymer, (b) SAXS profile for AB (AB-4) type diblock copolymer with reflection positions of assumed lamellar morphology. (c) Lorentz-corrected 1D SAXS profiles of (AB-4) di- and (ABA-2) triblock copolymers.



**Figure 7.** (a) Visibility without block copolymer film. (b) Visibility through transparent PMMA-*b*-PEHA-*b*-PMMA triblock copolymer film.

scattering maximum was observed in case of AB diblock copolymer indicating a general phase separation. ABA triblock copolymer showed at least two structures, which indicates that it has ordered or mixed phase morphology. But, the second weak maximum does not fit to any expected morphology for block copolymers like lamellar or hexagonally close packed cylinders (HCPC). This corresponds also to the AFM images where none of the common morphologies can be seen but a rather continuous pattern of one phase in the matrix. However, we were more interested in verifying the principle phase-separated nature of the samples as this is relevant to explain the mechanical properties of the block copolymer. The main *d*-spacing values obtained for AB di- and ABA triblock copolymers via SAXS analysis were found to be 84 and 64 nm, respectively. Thus the enhancement in tensile properties of ABA triblock copolymer can be correlated with the results from SAXS analysis. An ordered nanophase separated structure in block copolymer is usually attributed to outstanding mechanical and optical properties.<sup>29</sup> The phase domain size also plays an important role. Inferior mechanical properties are observed for larger domain size.<sup>30</sup> In our case, ABA triblock copolymer exhibited lower *d*-spacing value than AB diblock copolymer as well as a more ordered morphology explaining the superior mechanical properties observed.

**Transparency of Block Copolymers.** The prepared block copolymers were transparent. Figure 7 shows a transparent triblock copolymer's sheet through which the TEXT is clearly visible. Figure 8 shows the percentage transmittance (*T*%) vs

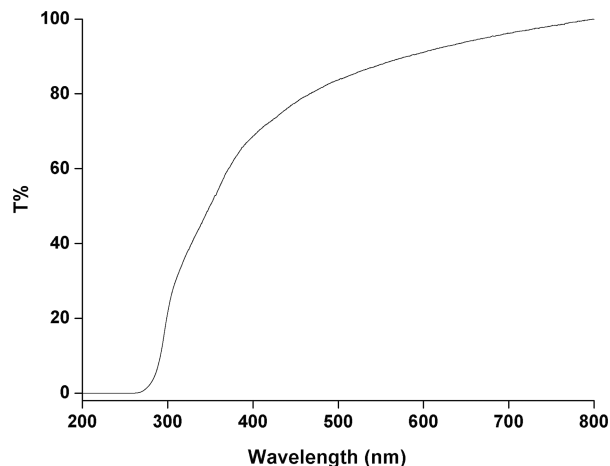


**Figure 8.** UV-visible spectrum of ABA triblock copolymer (ABA-2).

wavelength in the UV-visible spectrum of triblock copolymer. The block copolymer showed excellent transmittance in the visible region indicating its highly transparent nature. Formation of hard domain and soft domains did not affect the transparency in the acrylic block copolymers and thus it may be a potential material for transparent coatings or foils.

## CONCLUSIONS

AB and ABA type di- and triblock copolymers of EHA with MMA were prepared successfully based on a macroinitiator approach via ATRP. The presence of active -Br end groups in the PEHA macroinitiators was verified by <sup>1</sup>H NMR analysis and successful chain extension experiments. The prepared block copolymers were characterized by GPC analysis for molecular weight and molecular weight distribution which provided very good agreement between the theoretical and experimental  $M_n$  values and reasonable low dispersities. The molar percentage of individual monomer present in the block copolymers was determined by <sup>1</sup>H NMR analysis and was varied between 36 and 80 mol % MMA. DSC thermograms of the block copolymers showed two  $T_g$ 's corresponding to two domains present in the block copolymers. The tensile properties of these block copolymers were also evaluated and found to be enhanced with incorporation of longer PMMA segments which reinforced the tensile properties significantly especially in the ABA triblock copolymers. ABA block copolymer with 67 mol % MMA showed an excellent balance between high reinforcing effect of the PMMA hard domain and still relatively high elongation at break of 44%. The study showed clearly that the tensile properties of the block copolymers did not depend only on the PMMA content but it also depended strongly on the type of block copolymer. The tensile property of triblock copolymers was found to be significantly better than that of diblock copolymers. Morphological study of the block copolymers using SAXS and AFM analyses supported nanophase separated morphology for both block copolymers but a more ordered morphology and a smaller domain size for the triblock copolymers. Thus, it can be concluded that for a given PMMA/PEHA ratio, the triblock structure provides a more favorable bulk morphology in order to achieve good mechanical properties. However, the objective of this study was not just to compare the properties of AB and ABA type block copolymer but to evaluate the properties of this new type of acrylic block copolymer based on PEHA, which may be potential material for thermoplastic elastomer and fuel-resistant transparent coatings and adhesives. The resulting mechanical properties combined with the very high transparency make those all-

acrylate triblock copolymers highly interesting for tough and hard coatings or foils.

## ■ ASSOCIATED CONTENT

### ■ Supporting Information

<sup>1</sup>H NMR spectra of bifunctional macroinitiator and diblock copolymer, GPC traces of monofunctional macroinitiator and diblock copolymer, DSC traces of diblock and triblock copolymers and TGA and DTG plots of diblock and triblock copolymers. This material is available free of charge via the Internet at <http://pubs.acs.org/>.

## ■ AUTHOR INFORMATION

### Corresponding Author

\*E-mail: [nks@rttc.iitkgp.ernet.in](mailto:nks@rttc.iitkgp.ernet.in). Tel.: +91 3222 283178. Fax: +91 3222 282700.

### Notes

The authors declare no competing financial interest.

## ■ ACKNOWLEDGMENTS

The authors are thankful to DST, New Delhi for financial support. Nikhil K Singha is thankful to DAAD, Germany for the fellowship. The authors gratefully acknowledge Mr. A. Janke and Mr. S. Chowdhuri of IPF Dresden, Germany, for their help in the analysis of few samples.

## ■ REFERENCES

- (1) Hadjichristidis, N.; Pispas, S.; Floudas, G. *Block Copolymers: Synthetic Strategies, Physical Properties, And Applications*; John Wiley & Sons: Chichester, U.K., 2002.
- (2) Miguel, V. S.; Limer, A. J.; Haddleton, D. M.; Catalina, F.; Peinado, C. *Eur. Polym. J.* **2008**, *44*, 3853–3863.
- (3) Bonilla, A. M.; Haddleton, D. M.; Cerrada, M. L.; Garcia, M. F. *Macromol. Chem. Phys.* **2008**, *209*, 184–194.
- (4) Bonilla, A. M.; Haddleton, D. M.; Cerrada, M. L.; Garcia, M. F. *J. Polym. Sci., Part A: Polym. Chem.* **2008**, *46*, 85–92.
- (5) Bonilla, A. M.; Garcia, M. F.; Haddleton, D. M. *Soft Matter* **2007**, *3*, 725–731.
- (6) Cavicchi, K. A. *ACS Appl. Mater. Interfaces* **2012**, *4*, 518–526.
- (7) (a) Kim, J. K.; Yang, S. Y.; Lee, Y.; Kim, Y. *Prog. Polym. Sci.* **2010**, *35*, 1325–1349. (b) Quemener, D.; Bonniol, G.; Phan, T. N. T.; Gignes, D.; Bertin, D.; Deratani, A. *Macromolecules* **2010**, *43*, 5060–5065.
- (8) Brydson, J. A. *Rubbery Materials and Their Compounds*; Elsevier Applied Science: London, U.K., 1988.
- (9) Tang, X.; Gao, L.; Fan, X.; Zhou, Q. *J. Polym. Sci., Part A: Polym. Chem.* **2007**, *45*, 2225–2234.
- (10) Shipp, D. A.; Wang, J. L.; Matyjaszewski, K. *Macromolecules* **1998**, *31*, 8005–8008.
- (11) Chatterjee, U.; Jewrajka, S. K.; Mandal, B. M. *Polymer* **2005**, *46*, 10699–10708.
- (12) Grubbs, R. B.; Dean, J. M.; Bates, F. S. *Macromolecules* **2001**, *34*, 8593–8595.
- (13) Bae, B.; Miyatake, K.; Watanabe, M. *ACS Appl. Mater. Interfaces* **2009**, *1*, 1279–1286.
- (14) Ramakrishnan, A.; Dhamodharan, R. *Macromolecules* **2003**, *36*, 1039–1046.
- (15) Dayananda, K.; Ramakrishnan, A.; Dhamodharan, R. *J. Macromol. Sci Pure Appl Chem.* **2005**, *A42*, 471–484.
- (16) Mosnacek, J.; Yoon, J. A.; Juhari, A.; Koynov, K.; Matyjaszewski, K. *Polymer* **2009**, *50*, 2087–2094.
- (17) Fei, P.; Cavicchi, K. A. *ACS Appl. Mater. Interfaces* **2010**, *2*, 2797–2803.
- (18) Masař, J. K. B.; Tuzar, J. P. Z.; Pospíšil, H.; Doskočilova, D. *Macromolecules* **1998**, *31*, 41–51.
- (19) Tong, J. D.; Jerome, R. *Polymer* **2000**, *41*, 2499–2510.

- (20) Dufour, B.; Koynov, K.; Pakula, T.; Matyjaszewski, K. *Macromol. Chem. Phys.* **2008**, *209*, 1686–1693.
- (21) Vidts, K.; Dervaux, B.; Prez, F. Du. *Polymer* **2006**, *47*, 6028–6037.
- (22) Zheng, R.; Liu, G.; Jao, T. C. *Polymer* **2007**, *48*, 7049–7057.
- (23) Street, G.; Illsley, D.; Holder, S. J. *J. Polym. Sci., Part A: Polym. Chem.* **2005**, *43*, 1129–1143.
- (24) Qin, S.; Saget, J.; Pyun, J.; Jia, S.; Kowalewski, T.; Matyjaszewski, K. *Macromolecules* **2003**, *36*, 8969–8977.
- (25) Datta, H.; Singha, N. K. *J. Polym. Sci., Part A: Polym. Chem.* **2008**, *46*, 3499–3511.
- (26) Beers, K. L.; Matyjaszewski, K. *J. Macromol. Sci. Part A. Pure Appl. Chem.* **2001**, *38*, 731–739.
- (27) Kavitha, A. A.; Singha, N. K. *Macromolecules* **2010**, *43*, 3193–3205.
- (28) Haloi, D. J.; Singha, N. K. *J. Polym. Sci., Part A: Polym. Chem.* **2011**, *49*, 1564–1571.
- (29) Adhikari, R.; Michler, G. H. *Prog. Polym. Sci.* **2004**, *29*, 949–986.
- (30) Speckhard, T. A.; Gibson, P. E.; Cooper, S. L.; Chang, V. S. C.; Kennedy, J. P. *Polymer* **1985**, *26*, 55–69.
- (31) Tong, J. D.; Jerome, R. *Polymer* **2000**, *41*, 2499–2510.
- (32) Tong, J. D.; L. Ph.; Doneux, C.; Bredas, J. L.; Lazzaroni, R.; Jerome, R. *Polymer* **2001**, *42*, 3503–3514.
- (33) Datta, H.; Bhowmick, A. K.; Singha, N. K. *Polymer* **2009**, *50*, 3259–3268.
- (34) Haloi, D. J.; Ata, S.; Singha, N. K. *Ind. Eng. Chem. Res.* **2012**, *51*, 9760–9768.
- (35) Brooks, N. W. J.; Unwin, A. P.; Duckett, R. A.; Ward, I. W. *J. Macromol. Sci., Part A: Phys.* **1995**, *34*, 29–54.
- (36) Haloi, D. J.; Naskar, K.; Singha, N. K. *Macromol. Chem. Phys.* **2011**, *212*, 478–484.
- (37) Cowie, M. G. *Polymers: Chemistry & Physics of Modern Materials*; Blackie Academic & Professional: Glasgow, UK, 1991; p 337.